ULTIMATE LOAD TEST OF A SEGMENTALLY CONSTRUCTED PRESTRESSED CONCRETE I–BEAM

Saad E. Moustafa
Manager, Engineering Mechanics
Concrete Technology Corporation
Tacoma, Washington

Test results of a segmentally constructed prestressed concrete bridge I-beam are presented. The test girder was manufactured from short precast segments which were joined together and post-tensioned, after which a deck slab was cast on the top. The girder, 92 ft long, was cast in eleven segments: 9 segments of 8 ft each and two end blocks of 10 ft each. The assembled girder was then post-tensioned using two bonded tendons. The girder was made composite with a 6-in. thick, 6-ft wide, cast-in-place deck slab. The composite girder was then load tested, predominantly in flexure and its behavior, under working, cracking, and ultimate loads is reported. It is concluded that the performance of the segmentally constructed girder, under service as well as ultimate load, is comparable to that of a monolithic girder.

Spans of precast prestressed concrete bridge girders have been limited by the maximum transportable weights and/or lengths, rather than their capacities. When delivered over highways, the length of precast girders is usually limited to 100 ft maximum.

However, span capabilities of up to 250 ft can be achieved with existing standard cross sections.[1] Through segmental construction techniques, one can overcome existing limitations of weight and length and make possible more efficient use of the material.

Precast concrete segmental box girder bridges, with spans up to 300 ft, have been built; and spans of 750 ft can be constructed.[2] Glaidesville bridge, Sydney, Australia, is a segmental precast concrete post-tensioned arch bridge of 1000 ft span.

Segmental bridge construction involves the manufacture of precast concrete elements which are assembled at the job site. These units are joined together, end to end, and post-tensioned to form complete spans.

The length and weight of the segments are chosen so as to be most suitable for transportation and erection. Box girder and I-beam shapes have been used successfully. Efficient precasting techniques have been developed to produce elements with precise dimensions, well adapted to field assembly and jointing.

Very satisfactory joints between elements have been obtained by the use of epoxy resin as well as cement mortar and cast-in-place concrete. With epoxy joints, precision is obtained by match-casting the segments, one against the other.

Although a relatively large number of prestressed concrete bridges have been built by the segmental method, little has been published concerning the structural behavior of segmental girders, especially under cracking and under ultimate load conditions.[3]

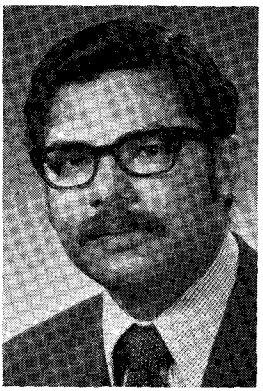

Saad E. Moustafa

SCOPE

This investigation was carried out for the purpose of reaching a better understanding of the behavior of segmentally constructed precast post-tensioned girders.

To achieve this objective, an experimental investigation was carried out as follows:

A bridge I-beam was cast in 11 segments. The segments were glued end to end. The assembled beam was then post-tensioned and the tendons grouted. Later, a deck slab was cast composite with the beam. The composite section was then load tested to failure. Elastic, as well as nonelastic, behavior of the beam was observed.

CROSS SECTION

The beam cross section at midspan, shown in Fig. 1-a, is known as the WSHD* Standard 100-ft Series. In

* Washington State Highway Department.

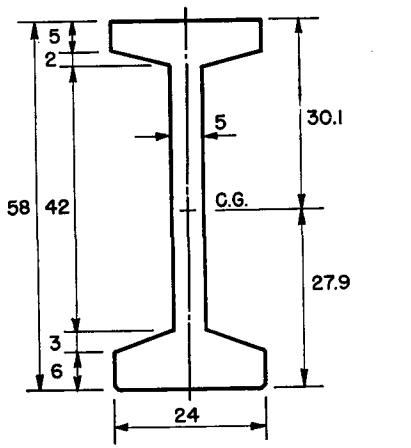

Fig. 1a. Typical cross section.

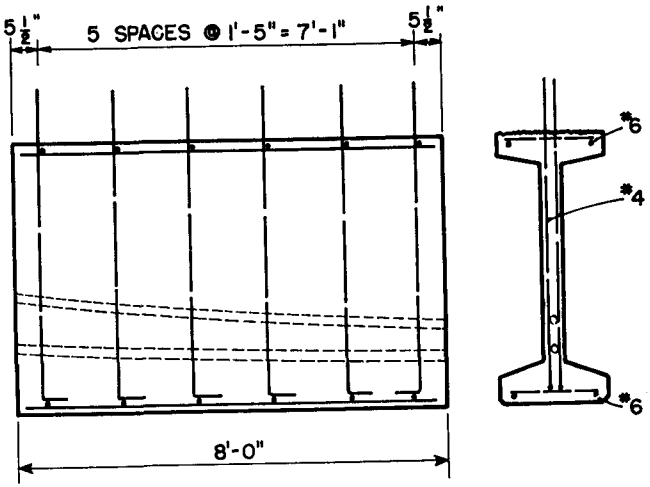

Fig. 1b Reinforcing details of typical segment.

practice, this beam is used for highway bridges in which a cast-in-place concrete deck is assumed to act composite with the beams for live loads.

The experimental girder was designed to satisfy AASHO† specifications[4] for prestressed concrete bridges carrying HS 20-44 loading, and required twenty-four 0.5-in. diameter, 270-kip post-tensioned bonded strands.

Two draped tendons of twelve ½-in., 270-kip strands each were used. Fig. 2 shows an elevation of the completed girder.

The overall length was 92 ft composed of 11 segments. Nine segments,

† American Association of State Highway Officials.

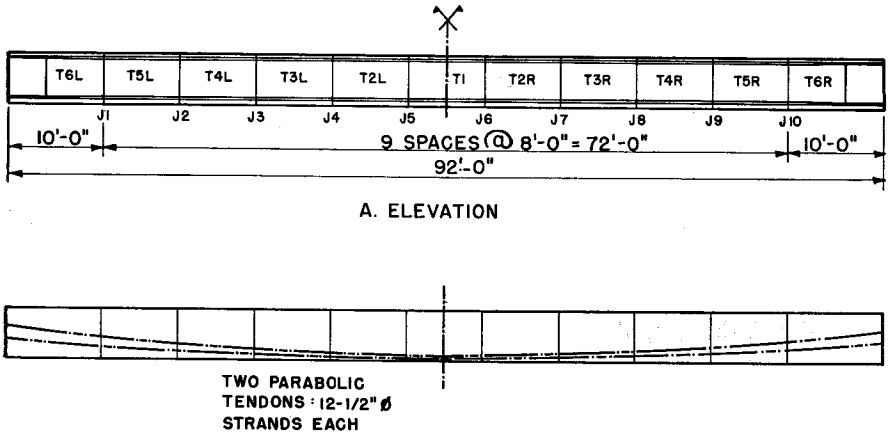

Fig. 2. Assembled girder.

8 ft each, were typical in cross section. Each segment was reinforced longitudinally with two No. 6 deformed bars in the bottom flange to minimize cracking under load in the segments and to force cracks to occur at the joints (see Fig. 1-b).

The webs of the two end segments were thickened to accommodate the post-tensioning anchors. Design calculations are presented in the Appendix.

FABRICATION AND MATERIALS OF SEGMENTS

A 20-ft steel form was used for casting the nine typical segments. The midspan segment T 1 was cast first and later moved to the left end of the form. Next, Segment T 2R was cast against the right end of Segment T 1.

This process was repeated with each

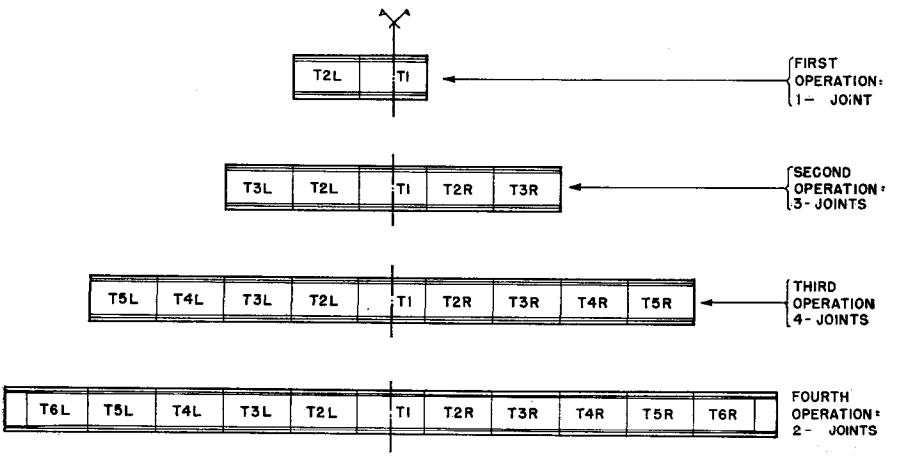

Fig. 3. Sequence of assembly.

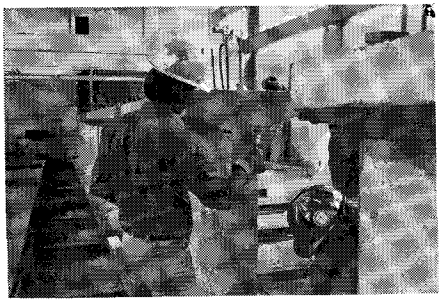

Fig. 4. Epoxy application.

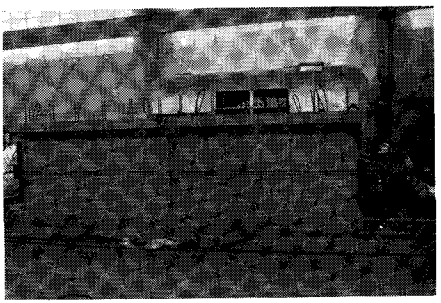

Fig. 5. First joint completed.

successive segment match-cast against its neighbor. A water-soluble form oil was used as a bond breaker, both on the surface of the form and on the end of each segment.

Both ends of each segment were prepared for gluing by sandblasting and cleaning any traces of form oil or loose particles. The 28-day cylinder strength of the concrete averaged 7500 psi.

ASSEMBLY OF SEGMENTS

In order to test the joint itself without any help from shear keys or alignment pins, the segments were cast with flat smooth ends. The segments were placed on a level base to assure proper alignment during the epoxy gluing operation. See Figs. 3 through 5, which illustrate the assembly procedure.

Manufacturer's data indicated that the pot life of the epoxy was 25 minutes. A layer of epoxy-sand mortar, about 1/16 to 1/8 in. thick, was applied on each of the mating surfaces.

When segments were forced together, mortar oozed out along the perimeter, insuring the absence of air voids in the joint. Temporary external prestressing of about 100 psi was applied immediately after each gluing operation and then released after 24 hours.

It should be noted that the elimination of shear keys and alignment pins did not affect the gluing operations, since each segment was resting on bunks. However, in the case of cantilever type of construction, where the use of aligning jigs is impossible, it is felt that shear keys should be provided.

To determine the shear strength of epoxy joints, small test beams made from 6-in. cubes, as shown schematically in Fig. 6, were prepared in the same way as the segmental girder.

The loading was applied in such a way as to force a failure in pure shear at the joints. Failure always occurred in the concrete layer adjacent to the epoxy.

As can be seen from Fig. 6, the shear strength increased from 1130 to 1900 psi when the normal prestress was increased from zero to 400 psi. From these results, it was concluded that the tensile strength of the joint is more critical than the shear strength.

POST-TENSIONING

After the last epoxy joint was 24 hours old, the temporary clamping cables were removed, and the tendons, each consisting of twelve 0.5 in. diameter 270-kip strands, were threaded through the ducts inside the assembled girder. A jacking force of 372 kips was applied at one end of each tendon.

The final elongation of the strands

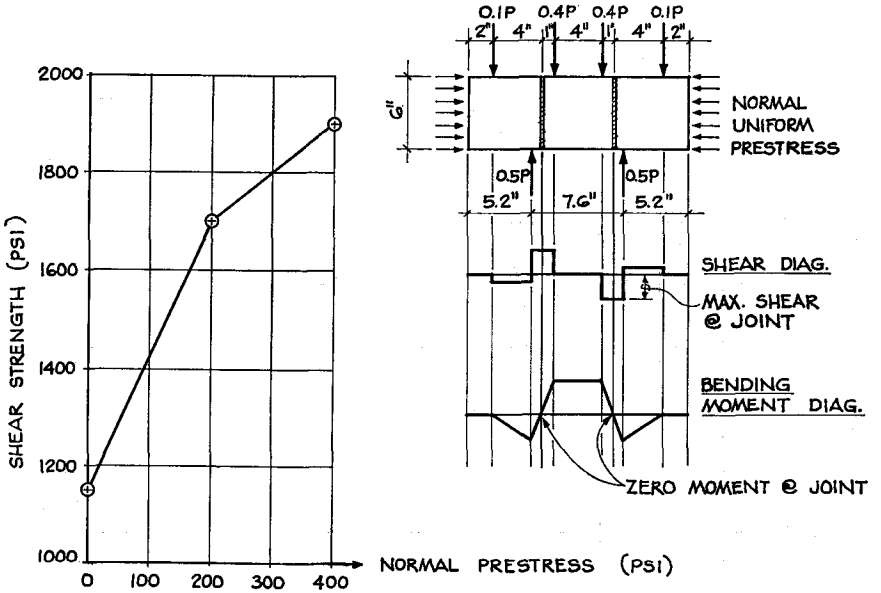

Fig. 6. Shear strength of epoxy mortar joints.

after seating the anchor was 7.0 in. Based on the jacking load and measured elongation, coefficients of wobble and friction were determined to be $k = 0.0002$ and $\mu = 0.20$, respectively.

Based on these friction loss coefficients, the effective prestress force transmitted at midspan was 653.5 kips. The measured instantaneous camber, at midspan, was 0.74 in.

Immediately after completion of the post-tensioning operation, the tendons were grouted using a neat cement mortar. Two days later, the girder was placed in its final position on the supports, where neoprene bearing pads were used.

DECK SLABS

The deck slab formwork was bolted to the girder. The dead weight of the deck slab was carried by the bare girder section alone. Interface shear between the girder and the deck slab was developed by projecting steel from the girder web and anchoring it into the slab.

The deck concrete had a 28-day cylinder strength of 5500 psi.

CAMBER HISTORY

The deck slab was cast 8 days after post-tensioning and grouting. During this time, the camber in the girder increased by 0.06 in., i.e., a total camber of 0.8 in. was measured prior to casting.

Immediately after casting, the girder deflected downward 0.42 in. under the dead weight of the wet concrete. Three hours after placing the deck concrete, the girder camber gradually increased until it stabilized after 12 hours. Shortly thereafter, the girder started to decrease its camber.

This phenomenon becomes intelligible if one realizes that the heat of hydration generated in the deck slab would raise the temperature of the top flange and cause upward deflection. Af-

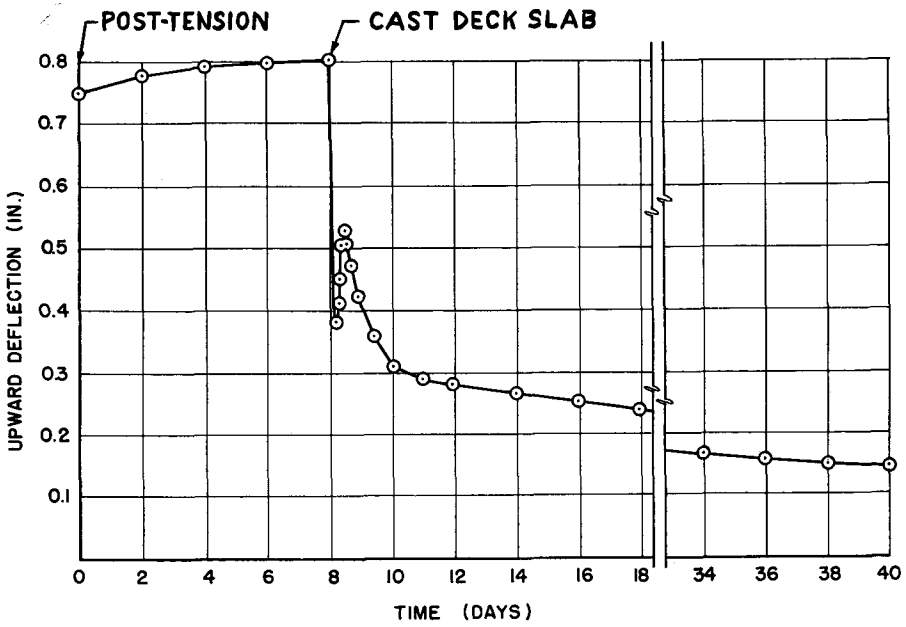

Fig. 7. Camber history.

ter the heat of hydration subsided, the girder deflected downward again.

Later, shrinkage of the newly cast concrete, which was partially restrained by the girder, caused additional downward deflection. Fig. 7 shows the history of camber in the beam up to the start of the test.

TEST PROCEDURE AND INSTRUMENTATION

The load test program consisted of the following four phases:

1. Evaluation of elastic constants.
2. Study of elastic behavior under service load.
3. Study of post-cracking nonelastic behavior under several levels of overload.
4. Evaluation of ultimate strength.

The live load on the beam simulated three concentrated axle loads from an AASHO HS 20-44 truck and trailer. The girder live load, plus impact, was applied by hydraulic jacks (see Fig. 8). The dead overload was simulated by 4300-lb concrete blocks.

One side of the girder was sprayed with a white latex paint to facilitate observation and recording of crack patterns. As each crack developed, it was marked in black.

Strains were measured mechanically, using an extensometer having an 8-in. gage length, and electrically, using SR-4 electric resistance bonded gages of 1-in. gage length.

Deflections were measured at each support, at midspan, and at one-quarter span. Deflections were measured by dial gages under the soffit and also by a precision level.

Crack widths were measured using a Bausch and Lomb 7-power microscope. Beam end rotation was measured by an inclinometer, which indicated angle rotations to the nearest 0.001 radians.

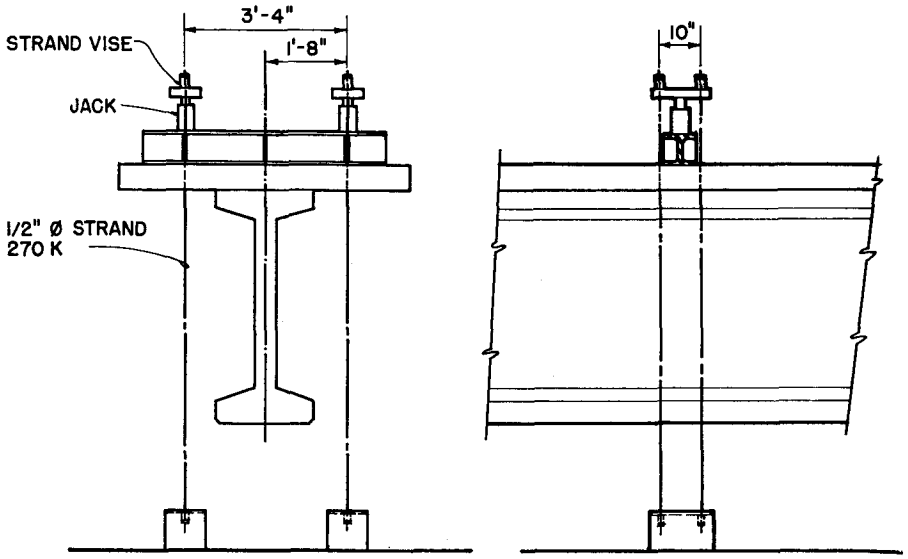

Fig. 8. Loading system detail.

TEST RESULTS AND DISCUSSION

Phase I

In order to evaluate the elastic constants, the girder was subjected to five increments of loading. Each load increment consisted of a concrete block weighing about 4300 lbs. Blocks were placed in the sequence and locations shown in Fig. 9.

The theoretical deflection was computed in terms of E (modulus of elasticity) for each load increment. Fig. 10 shows the computed values of $E\ \delta$ versus the measured values of δ. Using the least squares method, a value of E equal to 6480 ksi was obtained.

Phase II

The second phase loading consisted of two parts, a dead load and a live load part. The dead load represented

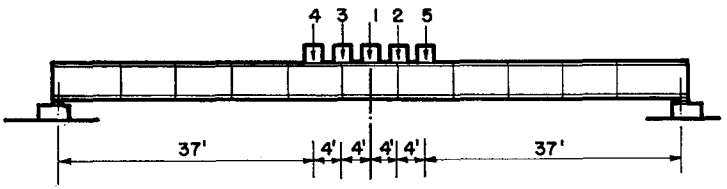

Fig. 9. Phase I loading sequence.

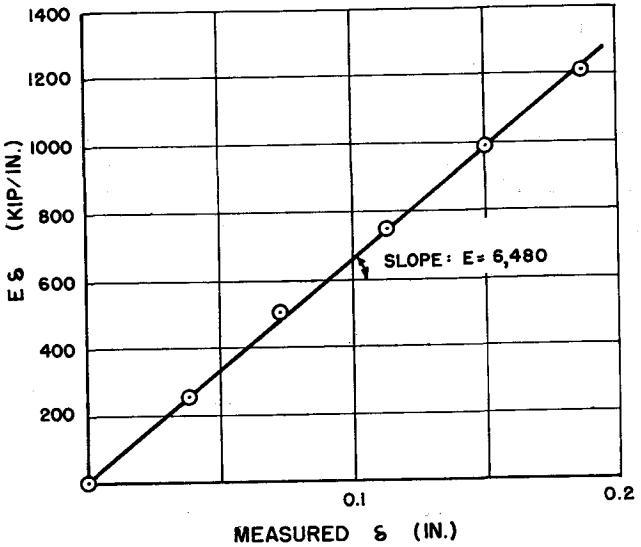

Fig. 10. Computed modulus of elasticity times deflection versus measured deflection.

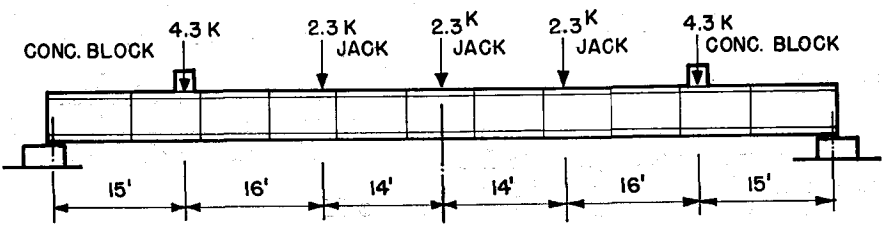

Fig. 11. Additional dead load.

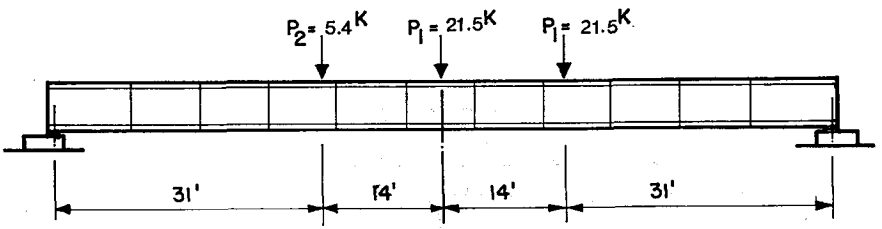

Fig. 12. Live load and impact factor.

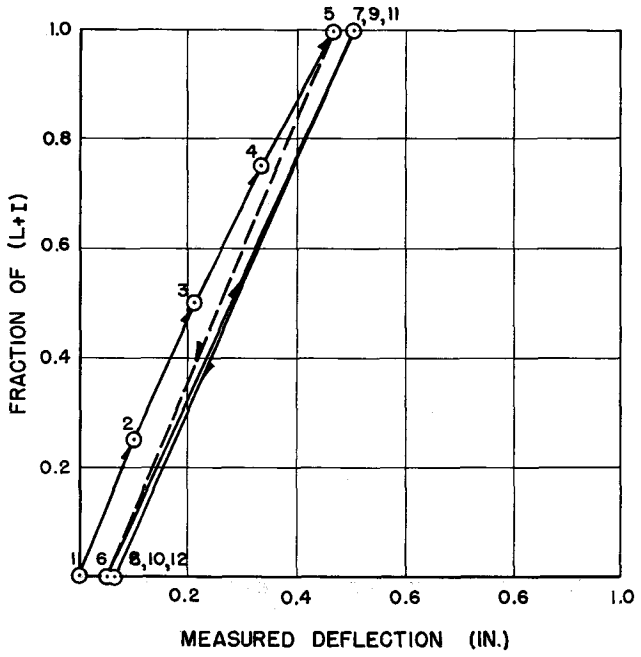

Fig. 13. Load versus midspan deflection.

the beam's share of the dead weight of the curbs, railings, diaphragms, and asphalt surface.

This additional dead load amounted to 15.5 kips, and was applied by two concrete blocks and hydraulic jacks, as shown in Fig. 11.

The live load which represented the beam's share of AASHO HS 20-44 truck load plus impact was applied by hydraulic rams, as shown in Fig. 8.

In order to produce the maximum live load bending moment in the beam at midspan, axle loads with locations and magnitudes shown in Fig. 12 were used. This load was applied in four equal increments and then removed.

Following this, the full load was applied and removed three times, and the load-deflection relations are plotted on Fig. 13.

The value of E obtained from the last three load cycles was 6050 ksi.

The computed neutral axis location and composite section properties assuming $E_{slab}/E_{girder} = 0.80$ are:

$$Y_b = 42.0 \text{ in.}, \; Y_t = 22 \text{ in.}$$

$$I = 453{,}500 \text{ in.}^4$$

$$Z_t = \frac{453{,}500}{(22)(0.80)} = 25{,}750 \text{ in.}^3$$

$$Z_b = \frac{453{,}500}{42} = 10{,}800 \text{ in.}^3$$

The computed fiber stresses under full live load, plus impact, are as follows:

$$f_t = \frac{M}{Z_t} = \frac{10{,}830}{25{,}750} = 0.42 \text{ ksi (comp)}$$

$$f_b = \frac{M}{Z_b} = \frac{10{,}830}{10{,}800} = 1.00 \text{ ksi (ten)}$$

Fig. 14 shows the strain distribution measured at midspan under full live load plus impact. The observed neutral

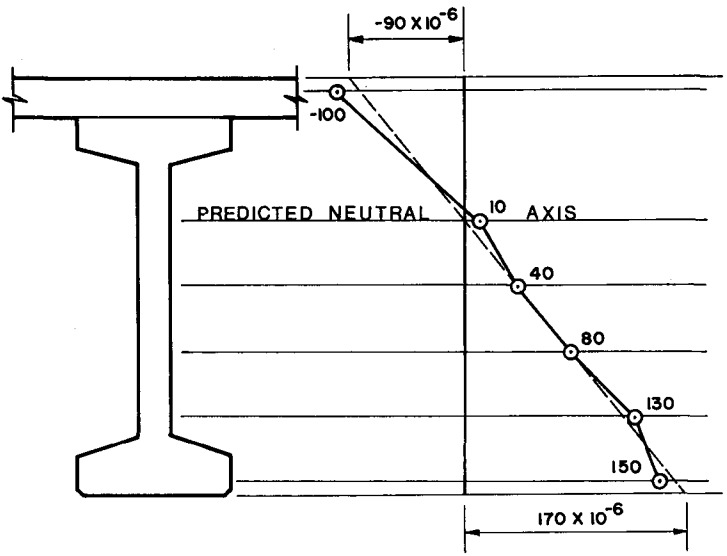

Fig. 14. Strain distribution at midspan under full design load.

axis location is about 1.5 in. above that computed.

Assuming the idealized strain distribution represented by the broken line, the following values of the moduli of elasticity for the girder and the slab are obtained:

$$E_{girder} = \frac{1.0}{170 \times 10^{-6}} = 5880 \text{ ksi}$$

$$E_{slab} = \frac{0.42}{90 \times 10^{-6}} = 4670 \text{ ksi}$$

The rotation of the ends of the girder was measured using the inclinometer.

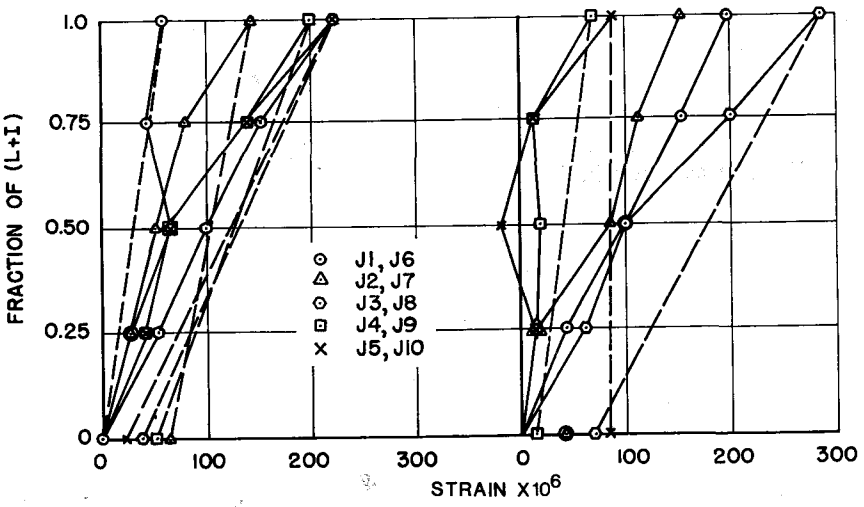

Fig. 15. Load versus strain across the joints.

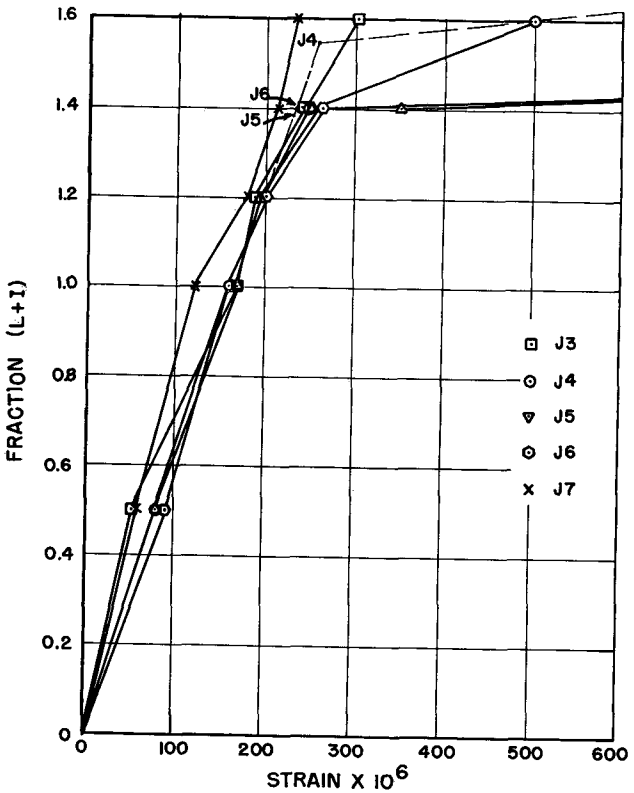

Fig. 16. Load versus strain across the joints (first cracking).

Under full live load plus impact, the angle of rotation was 0.015 radians, which indicated a value of E of 5716 ksi.

Fig. 15 shows the strains measured across the joints under load. An average value of E of 5800 ksi was calculated from these readings.

Comparing the three values of E obtained from three different types of measurement, a range of 5.5 percent was obtained.

Phase III

In this phase, the behavior of the girder under moderate overloads was studied. The live load was applied to the girder in increments until several cracks appeared in the bottom flange.

Cracks were detected at Joints 4, 5, and 6. The load, which reached 1.6 $(L + I)$, was then removed. Strains measured across Joints 3, 4, 5, 6, and 7 are shown in Fig. 16.

The cracking load is obtained by interpolation, as shown in Fig. 16. Cracks developed at Joints 5, 6, and 4 under 1.39, 1.4, and 1.55 times $(L + I)$, respectively. It was noticed that these cracks occurred in the concrete layer adjacent to the epoxy.

The live load was applied again in increments until the cracks at Joints 4, 5, and 6 reopened. The load, which reached 1.4 $(L + I)$, was then removed. Measured strains across Joints number 3, 4, 5, 6, and 7 are shown in Fig. 17. The load corresponding to the

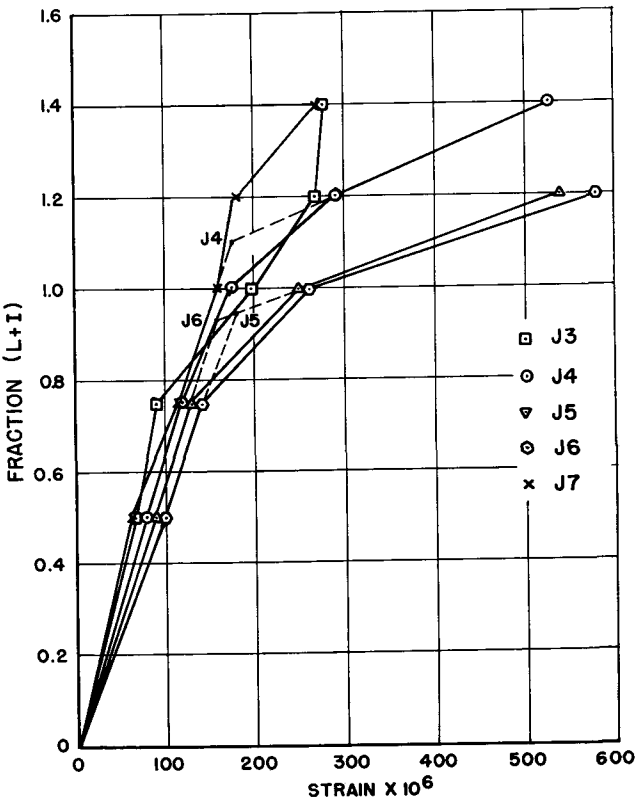

Fig. 17. Load versus strain across the joints (crack reopening).

reopening of each crack was determined by interpolation, as shown in Fig. 17.

Cracks reopened at Joints 6, 5, and 4 under 0.93, 0.94, 1.10 times $(L + I)$, respectively. At the instant of reopening of the cracks, the stress at the bottom fibers of the beam is zero.

Since the external loads are known, the amount of prestress left in the beam can be computed from equations of equilibrium and the condition of zero stress at the bottom fibers. Subtracting this force from the initial prestress force, the prestress loss can be estimated. The average prestress loss calculated from the above results was 9.3 ksi.

The bottom fiber stress increment corresponding to the difference between the loads causing initial cracking and those causing reopening of the cracks equals the tensile strength of the joint. The average value of the tensile strength obtained from the above results was 421 psi which corresponded to the tensile strength of the concrete adjacent to the joints.

Fig. 18 shows the load versus midspan deflection under these two load cycles. The occurrence and the reopening of the cracks can be seen from this figure. Note that the sensitivity of deflection to cracking is less than that of the strain across the joints.

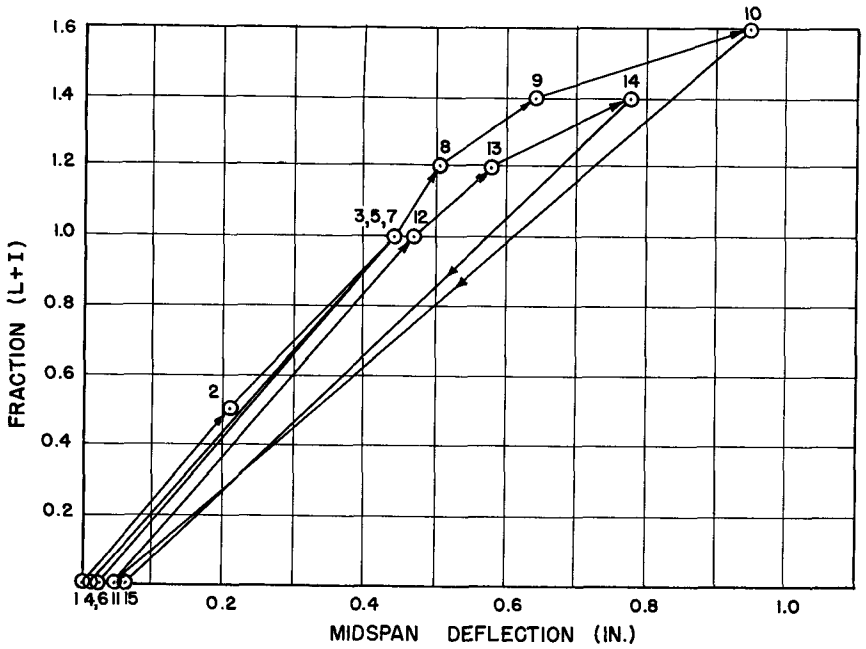

Fig. 18. Load versus midspan deflection.

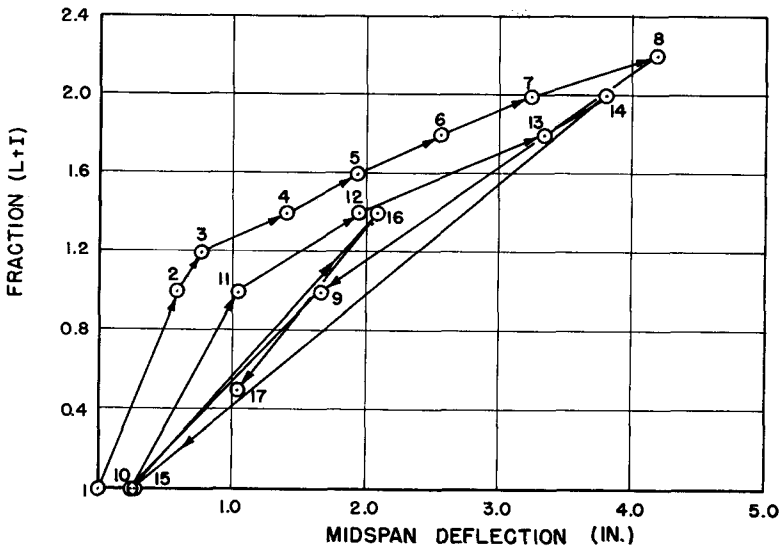

Fig. 19. Load versus midspan deflection.

After completion of the cracking load cycles, the beam was subjected to load cycles up to $[1.25D + 2.2\ (L + I)]$, equivalent to 2.65 $(L + I)$ in excess of its own weight.

Fig. 19 shows the load versus midspan deflections. Worth noting is the nearly complete recovery of deflection

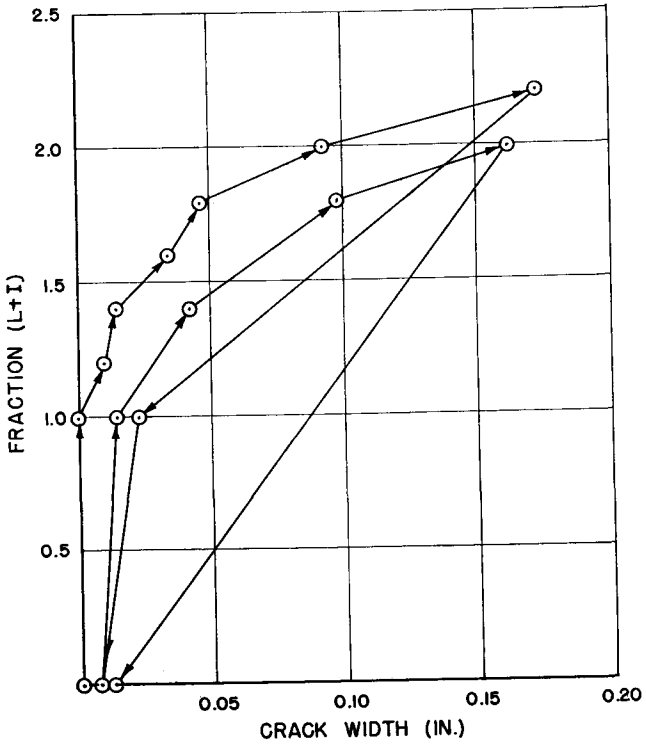

Fig. 20. Load versus crack width at J6.

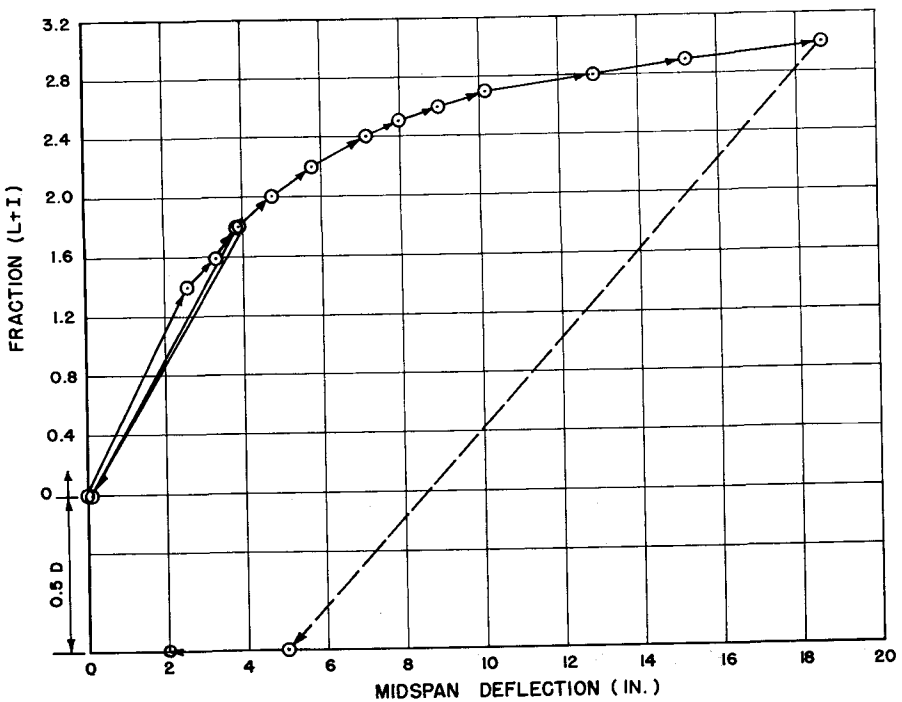

Fig. 21. Load versus midspan deflection.

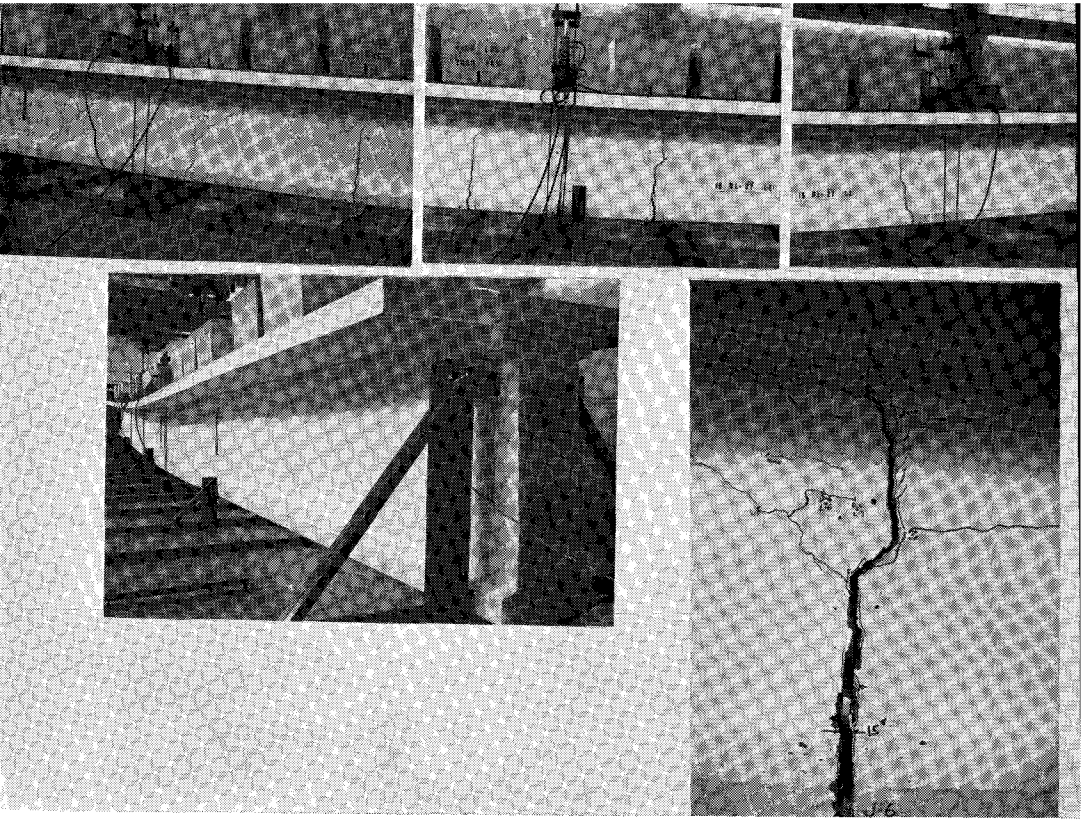

Fig. 22. Load test, August 1971.

after load removal, even under these high overloads. Fig. 20 shows load versus crack width across Joint 6.

Phase IV

Test of August 1971—The last loading phase was concerned with the ultimate strength of the girder. The additional dead load simulating the curb, railings, diaphragms, and asphalt surface, and 50 percent of all dead load were applied first in the form of concrete blocks. A total of 16 concrete blocks, each weighing 4.3 kips, was used.

The live load was applied by hydraulic jacks exactly in the same manner described in Phase III. It was planned to increase the live load monotonically until failure. However, when the total load reached $[1.5D + 3.0\ (L + I)]$, the deflection reached 18.5 in., which was the maximum possible under the test arrangement.

Upon release of the applied test load, the beam deflection recovered 13.5 in., leaving a residual deflection of 5 in., as shown plotted in Fig. 21. The beam was then stored for 2 years, during which time the deflection gradually decreased from 5 to 2 in.

Fig. 22 shows the beam during the progress of the test where it can be seen that cracks were localized at the joints. Consistently each crack progressed along the joint all the way up to the top flange in what can be described as flexural type cracking.

However, between one-half to two-thirds up the web height, shear flexural inclined cracks branched out from vertical cracks at joints near beam ends

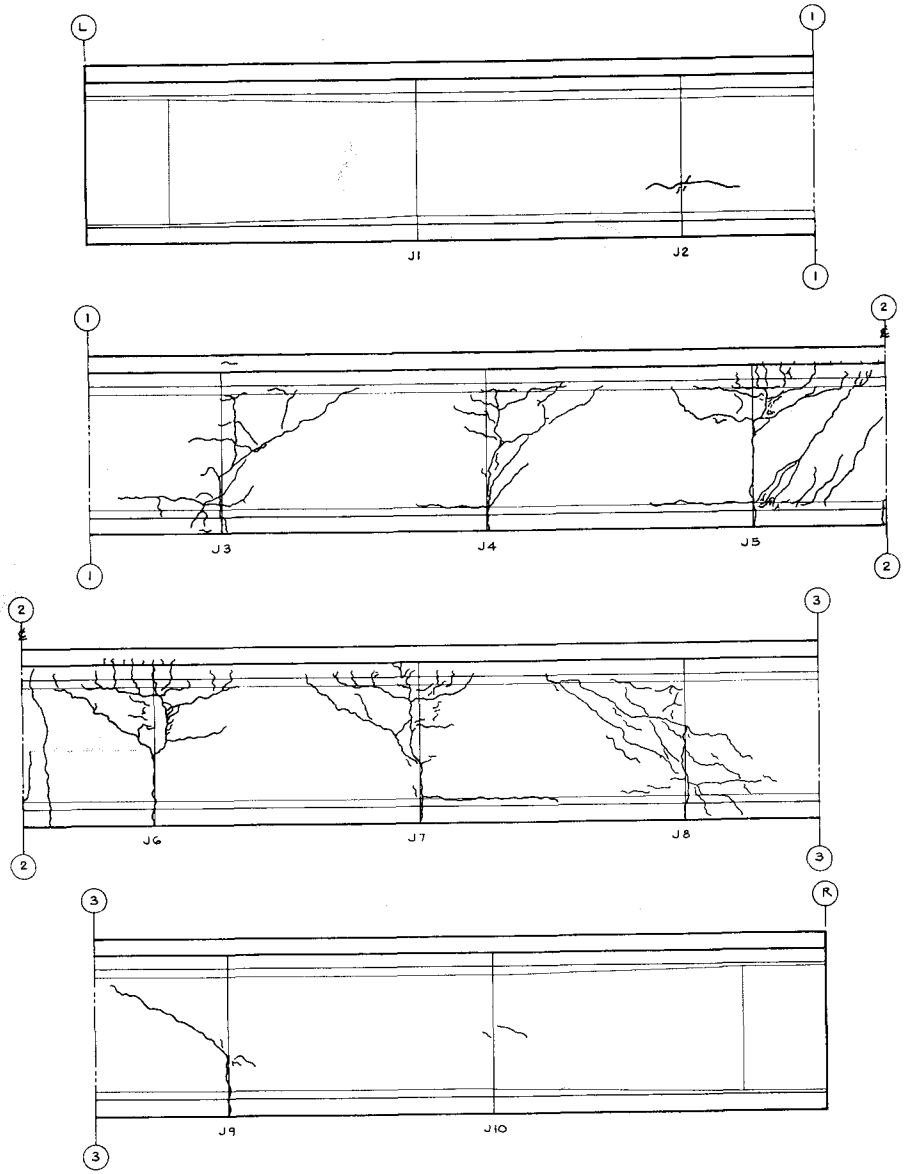

Fig. 23. Crack pattern.

(e.g., Joints 3 and 8). On the other hand, cracks near midspan at Joints 4, 5, 6, and 7 were more or less symmetrical in a tree-like pattern (see Fig. 23).

At maximum load level, the maximum crack width at Joint 6 was 1.5 in. and it could be seen propagating into the lower zones of the deck slab. This behavior indicated a tendency to concentrate the curvature and yielding of tendons at joint locations.

The amount of reinforcing steel in the bottom flange of each segment was insufficient to resist these high moments

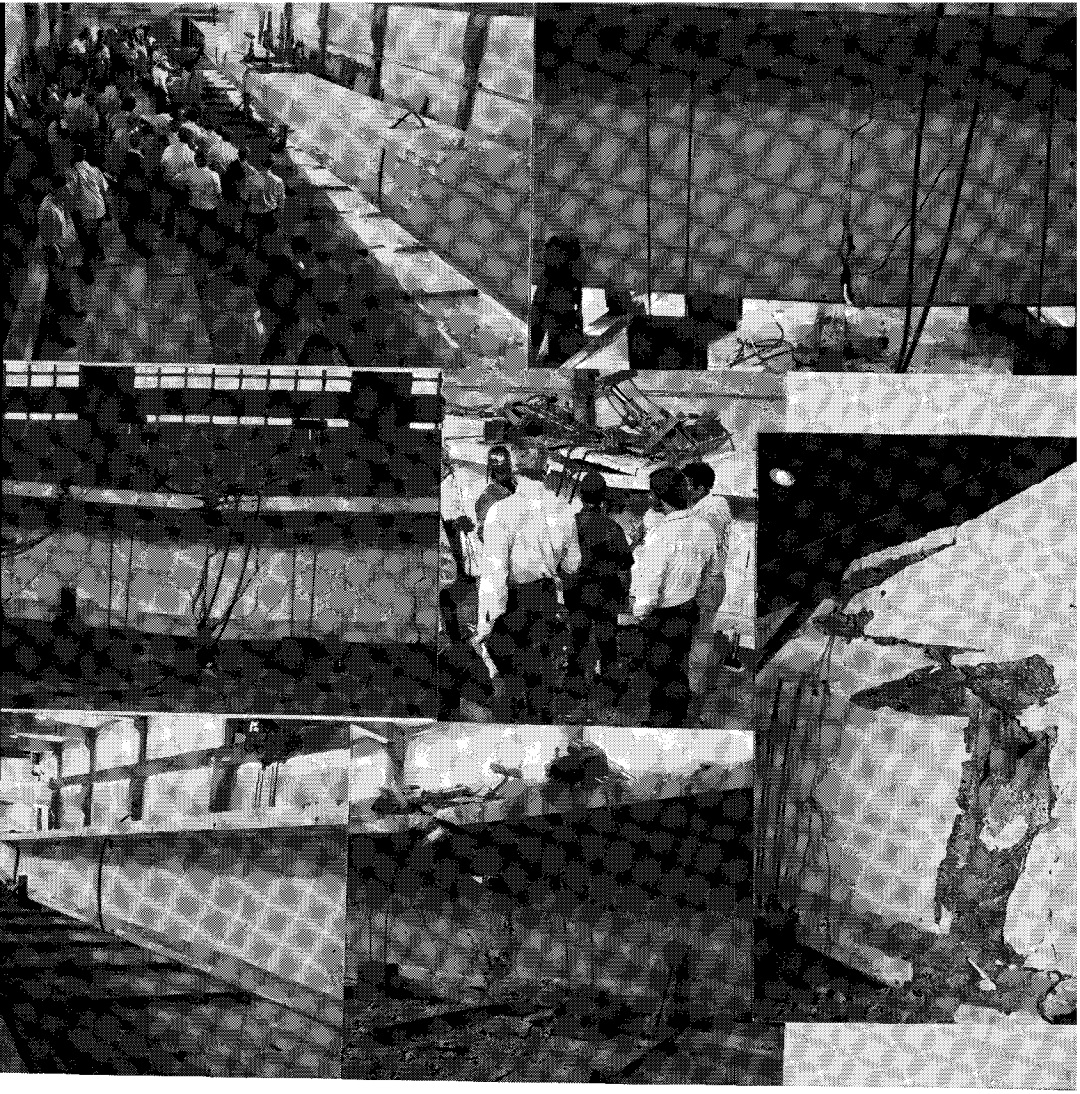

Fig. 24. Load test, September 1973.

without causing flexural cracking of the concrete in the lower flange. Consequently, the absence of this cracking indicated some loss of bond between the tendons and the bottom flange concrete. A computed curvature of 0.025 radians corresponded to a crack width of 1.5 in. and a neutral axis location 4 in. below the top of the deck.

If the curvatures were concentrated within the immediate vicinity of the joint, a compression failure in the flange would have occurred at an earlier stage of loading. The fact that the beam survived the load test intact can be explained by the spreading of the vertical crack into many branches (resembling a tree), as shown in Fig. 23.

The crack at Joint 6 (nearest midspan) ran upward to midheight of the web, and at a loading of $[1.25D + 2.2 (L + I)]$ the crack width reached 0.18 in. As the loading increased, two branches emerged from the single

crack, and subsequently spread into the tree-like pattern of Fig. 23. Obviously, the proliferation of cracks in the upper region of the beam caused a redistribution of curvature along the top flange.

It is believed that, while the placement of mild steel inside the bottom flange of the segments forced the cracking to take place at the joints, and the subsequent loss of bond between the prestressing tendons and the concrete prevented the initiation of new cracks in between, the continuous mild steel in the cast-in-place deck slab promoted the redistribution of strains and the development of the tree-like pattern of cracking. Therefore, the cast-in-place deck slab should be credited for the considerable ductility of the beam.

Test of September 1973—After 2 years of storage, the beam was again load tested, this time to destruction. The loading system consisted of two concentrated loads, one at midspan and the other 7 ft away. The ultimate load was reached when the top flange crushed.

A maximum concentrated load of 93 kips was reached at each load point before failure. This load exceeded the predicted value of 84.3 kips based on the procedure for calculating ultimate strength as given in Section 1.6.9 of the AASHO specifications.

The calculated procedure indicated a maximum tension stress in the prestressing tendons of 264 ksi at ultimate. Fig. 24 shows the beam during the progress of loading up to destruction.

The maximum load produced a bending moment corresponding to $[1.0D + 4.3\ (L + I)]$, or $[1.3D + 3.9\ (L + I)]$ loading.

A computed prestressing steel stress of 275.0 ksi corresponded to this load. A maximum compression strain of 0.0028 was measured in the top fibers before failure.

The exact location of the neutral axis at the instant of failure was not known; however, it is believed that a compression block of not more than 2 in. deep existed when the maximum load was acting on the beam, resulting in an average concrete stress of 7100 psi. The maximum recorded deflection before failure was 24 in.

CONCLUSIONS

Based on the observations and results obtained from this investigation, the following conclusions can be drawn:

1. Cracks occurred at the joints, as anticipated, due to the lack of any mild steel reinforcing bars in the joints between the segments.

2. Cracks at the joints occurred in the concrete adjacent to the epoxy mortar and the tensile strength of the epoxy exceeded that of the concrete.

3. Because the initial cracks were concentrated in the joints between the segments, one would assume some loss of ductility in the beam due to excessive hinging action of the top flange above the joint. However, the spreading of branch cracks in the webs at midheight caused a very favorable redistribution of compression along the top flange, resulting in ductile behavior at ultimate load.

4. The performance of the segmental beam exceeded the ultimate load criteria specified by AASHO for monolithic prestressed concrete construction. The concept of match-cast segments, glued together and post-tensioned is not only practical, but more than satisfies the technical requirements for highway bridges.

ACKNOWLEDGMENT

This investigation is part of a comprehensive research program on long span prestressed concrete bridges sponsored by Concrete Technology Corporation. The author gratefully acknowledges the guidance and technical assis-

tance of Dr. Arthur R. Anderson and Robert W. LaFraugh of Concrete Technology Corporation, Tacoma, Washington.

REFERENCES

1. Anderson, A. R., "Stretched-Out AASHO-PCI Beams, Types III and IV for Longer Span Highway Bridges," *PCI JOURNAL*, Vol. 18, No. 5, September-October 1973, pp. 32-49.

2a. Lee, D. J., "The Design of Bridges of Precast Segmental Construction," Table 1, *Technical Paper*, SfB Df(91), UDC 624.21:012.36, PCS 10, The Concrete Society Limited, Terminal House, Grosvenor Gardens, London SW1W oAU.

2b. Lee, D. J., "Prestressed Concrete Elevated Roads in Britain," *Technical Paper* SfB (91), UDC 652.-74.012.46 (41-4), PCS 12, The Concrete Society Limited, Terminal House, Grosvenor Gardens, London SW1W oAU.

2c. "Prestressed Viaducts Sweep Past Lake Geneva Hardly Harming a Tree," *Engineering News-Record*, January 8, 1970, p. 24.

2d. Lacey, G. C., and Breen, J. E., "Long-Span Prestressed Concrete Bridges of Segmental Construction, State of the Art," *Research Report* No. 121-1, The Texas Highway Department by Center for Highway Research, the University of Texas at Austin, May 1969.

3a. Somerville, G., and Caldwell, J. A. D., "Tests on a One-Twelfth Scale Model of the Mancunian Way," *Technical Report* SfB Ba4.-Ab5, UDC 624.74(427.2).001.5, TRA/394, Cement and Concrete Association, 52 Grosvenor Gardens, London SW1W oAU, December 1965.

3b. Leonhardt, Fritz, and Baur, Willi, "Die Agerbrucke eine aus Gros-Fertigteilen Zusammengesetzte Spannbetonbrucke," *Die Bautechnik*, Verlag von Wilhelm Ernst & Sohn, 1 Berlin 31, Hohenzollerndamm 169, July 1963.

3c. Hoving, H. T., Krijn, A. C., and van Loenen, J. H., "The Bridge Over the Oosterschelde," SfB(91) Du2, UDC 624.2.012.46 (492.6), Cement and Concrete Association, 52 Grosvenor Gardens, London SW1W oAU.

3d. Muller, Jean, "Precast Segmental Bridges Conception and Design Fundamentals," (Preprint), PCI Annual Convention (Chicago), September 23-27, 1973.

4. Standard Specification for Highway Bridges adopted by the American Association of State Highway Officials, Eleventh Edition, 1973.

APPENDIX—DESIGN CALCULATIONS OF TEST BEAM

The following design was performed in the summer of 1971, and, therefore, reflects the old AASHO Specifications load factors.

It should be pointed out, also, that the design is the same as that for monolithic contruction. No special reinforcement or prestressing is needed to account for stresses introduced during fabrication and assembly as is the case for cantilever construction.

1. Section Properties

Girder		Composite	
A	$= 546$ sq in.	Y^c_b	$= 42$ in.
Y_b	$= 27.9$ in.	I_c	$= 453{,}500$ in.^{4}
I	$= 249{,}000$ in.^{4}	Z^c_t	$= 25{,}750$ in.^{3}
Z_t	$= 8272$ in.^{3}	$Z_{I.F.}$	$= 28{,}344$ in.^{3}
Z_b	$= 8925$ in.^{3}	Z^c_b	$= 10{,}800$ in.^{3}

2. Loads

Girder:

$w = (546/144)\,(160) = 607$ lb/ft

$M = (0.607)\quad (90)^2\quad (1.5) = 7375$ in.-kips

Slab:

$w = (1)\ (6/12)\ (6.0)\ (150) = 450$ lb/ft
$M = (0.45)\ (90)^2\ (1.5) = 5470$ in.-kips
Asphalt, diaphragms, curb, and railing:
w (assumed) = 200 lb/ft
$M = (0.2)\ (90)^2\ (1.5) = 2400$ in.-kips
Live load (AASHO, HS 20-44):
Impact factor = $50/(125 + 90) = 0.23$
Live moment = 1345 ft.-kips
Girder moment plus impact =
$M_{L+I} = (1345)\ (12)\ (½)\ (6/5.5)\ (1.23)$
$= 10{,}830$ in.-kips

3. Estimate of required prestress

Moment acting on bare girder section =
$7375 + 5470 = 12{,}845$ in.-kips
Moment acting on composite section =
$2400 + 10{,}830 = 13{,}230$ in.-kips
Bottom fiber stress =
$f_b = (12{,}845/8925) + (13{,}230/10{,}800)$
$= 2.67$ ksi (tension)
Allowing no tension stress under full design load, then:
$P[(1/A) + (e/Z_b)] = f_b$
Assume $e = 27.9 - 4.25 = 23.65$ in.
Hence:
$P\ [(1/546) + (23.65/8925)] = 2.67$
from which $P = 596$ kips
Try two 12-½ in. diameter 270-kip strand tendons.

4. Friction loss calculation

Assume the tendons have a parabolic profile and let the distance from the soffit to the center of gravity of the tendons be X.
X at midspan = 4.25 in.
X at end = 29.25 in.
$X_{end} - X_{midspan} = 29.25 - 4.25 = 25$ in.
Angle $\alpha = (25)\ (8)/(90)\ (12)$
$= 0.185$ radians.
Assume a friction coefficient $\mu = 0.2$.
Also, assume a wobble coefficient
$K = 0.0002$ for semi-rigid smooth duct.
$(KL + \mu\alpha) = (90)\ (0.0002) + (0.2)\ (0.185)$
$= 0.055$
$f_{dead\ end} = f_{jacking\ end}\ e^{-(KL + \mu\alpha)}$
$= f_{j.e.}\ e^{-0.055} = 0.947\ f_{j.e.}$
$f_{j.e.} = (0.75)\ (270) = 202.5$ ksi
$f_{d.e.} = (0.947)\ (202.5) = 192$ ksi
Assume anchorage seating loss = 0.75 in.
Distance affected by seating loss:

$$X = \sqrt{\frac{(0.75)\ (90)\ (12)\ (28{,}000)}{(202.5 - 192)}}$$

$= 122$ ft (> 90 ft)

$$\text{Avg } \Delta f = \frac{(0.75)\ (28{,}000)}{(90)\quad (12)}$$

$= 19.4$ ksi

Therefore, $\Delta f_{j.e.} = 19.4 + 10.5 = 29.9$ ksi
and $\Delta f_{d.e.} = 19.4 - 10.5 = 8.9$ ksi

The effective prestress at mid-span equals $f_{j.e.}$ minus the friction and seating loss for the half-span minus the creep and shrinkage losses (25 ksi). Thus:
$f_{eff} = 202.5 - (10.5/2) - 19.4 - 25$
$= 153$ ksi
and
$P_{eff} = (153)\ (0.153)\ (24) = 561$ kips
(< 596 kips required)

However, since the beam will be tested a relatively short time after post-tensioning, only one-half of the losses due to shrinkage and creep will be considered. Therefore,
$f_{eff} = 153 + 12.5 = 165.5$ ksi
and
$P_{eff} = (165.5)\ (0.153)\ (24) = 608$ kips
[> 596 kips (ok)]

5. Tendon elongation

Before seating loss =

$$\frac{(202.5 + 192)\ (90)\ (12)}{(2)\quad (28{,}000)}$$

$= 7.61$ in.

After seating loss $= 7.61 - 0.75 = 6.86$ in.

6. Stress review

A summary of the working load stresses is given in Table 1.

Note: "c" denotes compression.
"t" denotes tension.

7. Ultimate strength check

M_u (req) $= 1.5\ D + 2.5\ (L + I)$
$= 1.5\ (7375 + 5470 + 2400)$
$+ 2.5\ (10{,}830)$
$= 49{,}943$ in.-kips
M_u (prov) $= A_s f_{su}\ d\ (1 - 0.6\ p f_{su}/f'_c)$
Now:
$f_{su} = 270\ [1 - (0.5)\ (0.00085)\ (270)/(5)]$
$= 263.8$ ksi
Therefore:
M_u (prov) $= (0.153)\ (24)\ (263.8)\ (59.75) \times$
$[1 - (0.6)\ (0.00085)\ (263.8)/(5)]$
$= 56{,}320$ in.-kips
[$> 49{,}943$ in.-kips (ok)]

Table 1. Summary of Working Load Stresses.

Stress conditions	Top fiber	Interface	Bottom fiber
$P/A = 608/546$		1.11c	1.11c
$Pe/Z = \frac{(608)\ (23.65)}{8272\ \&\ 8925}$		1.74t	1.61c
$M_{girder}/Z = \frac{7375}{8272\ \&\ 8925}$		0.89c	0.83t
$M_{slab}/Z = \frac{5470}{8272\ \&\ 8925}$		0.66c	0.61t
$M_{curb,\ .\ .}/Z = \frac{2400}{25750\ \&\ 28344\ \&\ 10800}$	0.09c	0.08c	0.22t
Service, dead load =	0.09c	1.00c	1.06c
$M_{L+I/Z} = \frac{10{,}830}{25750\ \&\ 28344\ \&\ 10800}$	0.42c	0.38c	1.00t
Service, full load =	0.51c	1.38c	0.06c

Note: "c" denotes compression.
"t" denotes tension.

8. Shear design

$$A_v = \frac{(V_u - V_c)\,S}{2\,f_y jd} \geq 0.0025 b's$$

$V_c = 0.06\,f'_c\,b'\,jd \leq 180\,b'\,jd$

Investigate shear at $L/4$:

V_u at $L/4 = (1.5)\ (90/4)\ (0.607 + 0.45 + 0.2) + (2.5)\ (31.2) = 121$ kips

$V_c = (0.18)\ (5)\ (0.8)\ (59.75) = 43$ kips

$$A_v = \frac{(121 - 43)\ (1)}{(2)\ (40)\ (0.8)\ (59.75)}$$

$= 0.0204$ in.²/in.

Use two No. 4 stirrups at 1 ft 7 in. full length.

9. Camber prediction

Prestress before creep and shrinkage losses $= (0.153)\ (24)\ (178) = 654$ kips

Moment due to post-tensioning at midspan $= (654)\ (23.65) = 15{,}460$ in.-kips

Eccentricity at end is practically zero.

$E_c = 33w^{1.5}\sqrt{f'_c}$

$= (33)\ (160)^{1.5}\ \sqrt{7500} = 5{,}784{,}000$ psi

Camber after post-tensioning =

$$\frac{(5)\ (15460 - 7375)\ (90)^2\ (12)^2}{(48)\ (5784)\ (249{,}000)}$$

$= 0.68$ in. (up)

Discussion of this paper is invited.
Please forward your discussion to PCI Headquarters by December 1, 1974, to permit publication in the January-February 1975 PCI JOURNAL.